

<https://helda.helsinki.fi>

Substantial large-scale feedbacks between natural aerosols and climate

Scott, Catherine

2017-12-04

Scott , C , Arnold , S , Monks , S , Asmi , A , Paasonen , P & Spracklen , D 2017 , ' Substantial large-scale feedbacks between natural aerosols and climate ' , Nature Geoscience , vol. 11 , no. 1 , pp. 44-48 . <https://doi.org/10.1038/s41561-017-0020-5>

<http://hdl.handle.net/10138/308161>

<https://doi.org/10.1038/s41561-017-0020-5>

unspecified

acceptedVersion

Downloaded from Helda, University of Helsinki institutional repository.

This is an electronic reprint of the original article.

This reprint may differ from the original in pagination and typographic detail.

Please cite the original version.

25 **negatively related to the observed global temperature anomaly, and is driven**
26 **by a positive relationship between temperature and emission of natural**
27 **aerosol. The extra-tropical aerosol-climate feedback is estimated to be -0.14**
28 **Wm⁻² K⁻¹ for landscape fire aerosol, greater than the -0.03 Wm⁻² K⁻¹ estimated**
29 **for biogenic secondary organic aerosol. These feedbacks are comparable in**
30 **magnitude to other biogeochemical feedbacks, highlighting the need for**
31 **natural aerosol feedbacks to be included in climate simulations.**

32

33 The terrestrial biosphere regulates atmospheric composition and climate by altering
34 the exchange of energy, water and trace gases between the surface and
35 atmosphere¹. The terrestrial biosphere is an important source of natural aerosols²
36 from vegetation fires and biogenic volatile organic compounds (BVOCs) which can
37 form secondary organic aerosol (SOA)³. These natural sources can dominate
38 ambient aerosol in tropical⁴⁻⁷, temperate^{8,9} and boreal¹⁰ environments. Atmospheric
39 aerosol alters the Earth's climate by absorbing and scattering radiation (direct
40 radiative effect) and through altering the albedo of clouds (first aerosol indirect
41 effect)¹¹. Because natural aerosol constitutes a major fraction of ambient aerosol it
42 can have important radiative effects¹²⁻¹⁵. The physical and biological process that
43 control natural aerosol sources are highly sensitive to climate². For example,
44 changes to climate drive large changes in fire¹⁶⁻¹⁸, BVOC¹⁹ and dust²⁰ emissions.
45 These interactions between natural aerosol and climate create the potential for
46 natural aerosol-climate feedbacks.

47 A number of natural aerosol-climate feedbacks have been proposed. The first
48 proposed, and maybe best known, involves ocean biology and emission of di-
49 methylsulfide²¹. Terrestrial aerosol-climate feedbacks have also been suggested¹.

50 Warmer temperatures drive increased BVOC emissions and increased SOA
51 concentrations, which lead to a negative radiative effect and a cooling impact on
52 climate²². Warmer temperatures also lead to increased fires and associated aerosol
53 emissions¹⁶ with impacts on climate. Observations of increased aerosol
54 concentrations with increasing ambient temperatures have been attributed to these
55 interactions^{23,24}. However, the magnitude of natural aerosol feedbacks has rarely
56 been assessed, although large projected changes in natural aerosol under a
57 warming climate suggest that they could be substantial². Here we explore the
58 potential magnitude of aerosol feedbacks for two terrestrial natural aerosol sources
59 with important climate impacts¹²: biogenic SOA and landscape fire aerosol.

60 **Exploring natural aerosol – temperature interactions**

61 To explore the potential for natural aerosol-climate feedbacks, we analysed long-
62 term measurements of aerosol number made at 11 continental locations
63 (Supplementary Fig. 1) mostly across northern hemisphere mid-latitudes²⁴. We used
64 the number concentration of particles with dry diameter larger than 100 nm (N_{100}) as
65 a proxy for concentrations of cloud condensation nuclei (CCN)²⁵. Particles with dry
66 diameters larger than 100 nm are also those that are able to scatter radiation
67 efficiently in the atmosphere.

68 At most of these locations, N_{100} is positively related to local surface temperature
69 (Supplementary Fig. 2) as reported previously²⁴. We find that a global aerosol
70 microphysics model²⁶ (see Methods) reproduces this observed relationship well
71 (Supplementary Fig. 2). To further explore the relationship between surface
72 temperature and N_{100} , we de-seasonalised both variables. Figure 1 shows the N_{100}
73 anomaly as a function of anomaly in local surface temperature. In summer we find
74 that most locations exhibit a strong positive relationship between temperature

75 anomaly and anomaly in N_{100} , with little or no relationship in winter. This means that
76 in summer, days that are warmer than average typically have higher than average
77 N_{100} . The global model, analysed in the same way as the observations, reproduces
78 the observed relationships (Fig. 1). The summertime mean observed sensitivity
79 between N_{100} and temperature, calculated across all observation stations, is
80 $+51.3 \pm 5.9 \text{ cm}^{-3} \text{ K}^{-1}$ (linear regression based on 500 bootstrap samples) and is well
81 reproduced by the model ($+43.5 \pm 4.2 \text{ cm}^{-3} \text{ K}^{-1}$). The relative anomaly in particle
82 number shows a similar relationship that is also well reproduced by the model
83 (Supplementary Fig. 3). This suggests that the model captures the processes
84 responsible for driving the observed temperature-aerosol relationships.

85 The observed relationship between temperature and aerosol number could be due to
86 interactions between natural aerosol sources and climate. However, it could also be
87 due to processes unrelated to natural aerosol sources. For example, warmer
88 temperatures could be associated with lower rainfall, and therefore reduced aerosol
89 loss via wet deposition. Or warmer temperatures could be related to transport of
90 southerly air masses towards the measurement locations, bringing more polluted air
91 with high aerosol concentrations.

92 To help interpret the observed relationships, we analysed multiple simulations from
93 the atmospheric aerosol model in which we individually switch off interannual
94 variability in natural aerosol emissions or meteorology (see Methods). At all
95 locations, we find that the simulated relationship between N_{100} anomaly and
96 temperature anomaly breaks down (sensitivity of N_{100} to temperature reduced to
97 $+5.0 \pm 1.6 \text{ cm}^{-3} \text{ K}^{-1}$) when we remove interannual variability in simulated meteorology
98 (i.e., the simulation uses repeating 1997 meteorological data). This suggests that
99 meteorology is an important mechanism driving the observed relationship between

100 anomalies in N_{100} and temperature. Simulations where we remove interannual
101 variability in natural aerosol emissions have less impact on the simulated relationship
102 between N_{100} and temperature, with sensitivity reducing to $+41.9 \pm 4.2 \text{ cm}^{-3} \text{ K}^{-1}$ for
103 fixed fire and $+40.9 \pm 4.0 \text{ cm}^{-3} \text{ K}^{-1}$ for fixed BVOC emissions (Supplementary Fig. 4).
104 We also find that if we increase simulated SOA formation from BVOCs (by a factor 5)
105 the relationship between N_{100} and temperature further breaks down at warm
106 temperature anomalies (Supplementary Fig. 4). This demonstrates that the
107 relationship between N_{100} and temperature is sensitive to the treatment of SOA in the
108 model and suggests that this treatment is adequately represented in the control
109 simulation. Overall our analysis suggests that whilst meteorology is the dominant
110 driver of observed relationships between temperature and aerosol number, variability
111 in natural aerosol emission also contributes. Our realistic simulation of the observed
112 relationships between aerosol and temperature suggests that our model treatment of
113 fire emissions and SOA¹⁴ are adequate to simulate the main interactions that are
114 important for this study.

115 **Interannual variability in aerosol radiative effects**

116 Using the multi-annual simulations of global aerosol, we explore how natural aerosol
117 sources alter the interannual variability in top-of-atmosphere aerosol radiative
118 effect. We focus on the aerosol direct radiative effect (DRE) and first aerosol indirect
119 effect (AIE), also known as the cloud albedo effect¹¹. Other interactions between
120 aerosol and cloud are likely, but are highly uncertain²⁷. Over the period 1997 to
121 2007, the global annual mean DRE has a standard deviation of 0.025 W m^{-2}
122 whereas the AIE has a standard deviation of 0.017 W m^{-2} (Supplementary Figure 5).
123 In this control simulation, year to year variability in fire emissions are prescribed from
124 the Global Fire Emissions Dataset version 3 (GFED3)²⁸ and BVOC emissions are

125 calculated using MEGAN version 2.1 (ref.²⁹). To isolate the contribution of different
126 aerosol sources to this variability in the aerosol RE we individually switch off natural
127 aerosol - climate couplings (see Methods). We then use the difference between the
128 control simulation and the simulation where the interannual variability of the natural
129 aerosol source has been switched off to calculate the variability caused by each
130 natural aerosol source. Figure 2 shows the interannual variability in simulated
131 aerosol RE due to variability in biogenic SOA and fire emissions. Variability in fire
132 aerosol causes interannual variability in both DRE and AIE of greater than 0.5 W m^{-2}
133 over and downwind of regions of tropical and boreal fires. Interannual variability in
134 biogenic SOA causes smaller variability in RE, with variability of up to 0.2 W m^{-2} over
135 the SE United States and tropical forest regions. Landscape fires have also been
136 shown to control interannual variability in regional surface carbonaceous aerosol
137 concentrations⁹ and aerosol optical depth³⁰.

138 Figure 2 shows that some of the largest simulated radiative impacts caused by
139 variability in natural aerosol are in the tropics. However, our understanding of
140 atmospheric composition and emissions of natural aerosol in the tropics is still poor.
141 There are very few long-term studies of aerosol size distribution in the tropical
142 atmosphere and none of our 11 stations are in the tropics (defined here as 20°S to
143 20°N). The tropics are thought to be the dominant source of both BVOC²⁹ and fire²⁸
144 emissions. However, there have been few studies of BVOC emissions in the tropics.
145 A study in the Amazon, confirmed the importance of temperature, light and leaf
146 phenology in driving BVOC emissions but also suggested our mechanistic
147 understanding of BVOC emissions in the tropics is still limited³¹. The chemical
148 composition of monoterpene emissions in the tropics may also vary with
149 temperature, with reactive isomers being enriched at high temperatures^{32,33} with

150 potential consequences for SOA. For these reasons we focus on the extra-tropical
151 ($>20^{\circ}\text{S}$ and $>20^{\circ}\text{N}$) RE, where there is less uncertainty in BVOC emissions and we
152 have observations to constrain the sensitivity of the aerosol model to natural aerosol.
153 We explored the control on the variability in aerosol RE over the period 1997 to 2007
154 (see Methods). We find that there is a negative correlation between global (land and
155 ocean) surface temperature anomaly and the anomaly in extra-tropical annual mean
156 DRE (Pearson's $r = -0.74$, $P < 0.01$) and AIE ($r = -0.52$, $P < 0.1$) (Supplementary Table
157 1). Figure 3 shows the anomaly in RE due to variability in biogenic SOA and fire
158 aerosol as a function of the anomaly in annual global temperature (see Methods).
159 We find an even stronger negative correlation between the global temperature
160 anomaly and anomaly in extra-tropical annual mean RE from biogenic SOA, both for
161 the DRE ($r = -0.76$, $P < 0.01$) and AIE ($r = -0.71$, $P < 0.01$). Simulated emissions of BVOC
162 are strongly controlled by temperature²⁹; we find a strong positive correlation
163 between annual extra-tropical BVOC emission and global temperature anomaly
164 (monoterpene $r = 0.78$; isoprene $r = 0.79$) (Supplementary Figure 7). Warmer than
165 average years drive increased BVOC emissions leading to increased formation of
166 SOA, which results in a stronger negative DRE and AIE.

167 We also simulate a negative correlation between global temperature anomaly and
168 the anomaly in the extra-tropical RE from fire, both for the DRE ($r = -0.5$, $P < 0.1$) and
169 AIE ($r = -0.51$, $P < 0.05$). We find a positive correlation between annual extra-tropical
170 particulate emission from landscape fires and global temperature anomaly ($r = 0.39$)
171 (Supplementary Fig. 7). The correlation between temperature anomaly and RE from
172 fires is weaker compared to BVOC, due to this weaker correlation between
173 temperature and fire emission. Global fire activity is governed by a complex suite of
174 climate, natural and human ignition sources and available fuel¹⁸. Whilst years with

175 warm temperature anomalies are associated with greater fire emissions, other
176 climate variables such as rainfall and relative humidity are also important^{18,34}.

177 **Diagnosing natural aerosol-climate feedbacks**

178 We used the relationship between RE and global temperature anomaly to estimate
179 the aerosol radiative feedback (λ) for the different natural aerosol sources, following
180 the framework of previous work¹ (see Methods). In this framework climate feedbacks
181 are expressed in common units of $W m^{-2} K^{-1}$ and are shown in Figure 4. We estimate
182 that fire results in an extra-tropical direct aerosol radiative feedback of $-0.09 \pm 0.06 W$
183 $m^{-2} K^{-1}$ and an extra-tropical indirect aerosol radiative feedback of $-0.06 \pm 0.03 W m^{-2}$
184 K^{-1} . We estimate a smaller radiative feedback due to biogenic SOA, with an extra-
185 tropical direct radiative feedback of $-0.02 \pm 0.01 W m^{-2} K^{-1}$ and an extra-tropical
186 indirect aerosol radiative feedback of $-0.007 \pm 0.002 W m^{-2} K^{-1}$.

187 Figure 4 also shows our estimates of the global radiative feedbacks. The global
188 aerosol feedback for fire aerosol is relatively similar to that calculated for the extra-
189 tropics. In contrast, the global biogenic SOA feedback is about double the strength of
190 that calculated in the extra-tropics (Fig. 4). We note that we have no observational
191 constraint of the natural aerosol feedback in the tropics, and so these global
192 estimates are unconstrained. Long-term observations of BVOC emissions and
193 aerosol concentrations in the tropics are urgently needed.

194 The stronger fire aerosol radiative feedback compared to the biogenic SOA feedback
195 is primarily due to the stronger interannual variability of fire emissions compared to
196 BVOCs. The coefficient of variation (standard deviation divided by mean) for global
197 particulate emission from fire is 19.6% (Supplementary Fig. 7 and Methods). The
198 simulated coefficient of variation for BVOC emissions is substantially smaller both for
199 isoprene emissions (2.9%) and for monoterpene emissions (2.4%). Our simulated

200 interannual variability in BVOC emissions and biogenic SOA matches previous
201 work³⁵. The absolute variability in both BVOC and particulate emissions from fire is
202 greatest in the tropics, but the extra-tropics exhibits greater fractional variability
203 (Supplementary Fig. 6 and 7).

204 We find that the direct radiative feedback is stronger than the indirect radiative
205 feedback for both natural aerosol sources. This behaviour is particularly true for
206 biogenic SOA where the direct aerosol feedback is more than a factor 3 greater than
207 the indirect aerosol feedback. We note that our estimated direct aerosol feedback for
208 fires will depend on the net DRE of fire aerosol which is uncertain³⁶. The relatively
209 weak aerosol indirect feedback for biogenic SOA is due to the AIE being relatively
210 insensitive to emission of BVOC^{12,14}. The global biogenic SOA feedback from
211 aerosol indirect effect that we estimate here ($-0.013 \pm 0.002 \text{ W m}^{-2} \text{ K}^{-1}$) is similar to
212 the global mean value of $-0.01 \text{ W m}^{-2} \text{ K}^{-1}$ inferred from selected observations²⁴.

213 Our estimate of natural aerosol - climate feedbacks is applicable for the present day
214 and may be different in future or past climates. Climate change and increased
215 atmospheric carbon dioxide concentrations will alter the amount and type of
216 vegetation^{37,38}, altering both BVOC²⁹ and fire emissions^{39,40}. Changes in
217 environmental factors in a warming climate may lead to stressed vegetation and
218 additional BVOC emissions, potentially creating stronger couplings between
219 vegetation, aerosol and climate⁴¹. Increased CO₂ concentrations may alter BVOC
220 emissions²⁹, altering biogenic SOA and associated feedbacks. Feedbacks can also
221 be directly altered by human activity. Land-use change and land management have
222 altered BVOC and fire emissions since pre-human times⁴². Anthropogenic aerosol
223 suppresses natural aerosol - climate interactions⁴³, meaning natural aerosol - climate
224 feedbacks may strengthen with future reductions in anthropogenic aerosol

225 emissions. Additional feedbacks between the biosphere, BVOC, fire emissions and
226 climate operating through precipitation and soil moisture are possible, but are not
227 included here.

228 The strength of natural aerosol feedbacks is comparable in magnitude to a range of
229 other biogeochemical feedbacks¹ and is opposite in sign to the global snow-albedo
230 feedback which has been estimated as $+0.1 \text{ W m}^{-2} \text{ K}^{-1}$ (ref.⁴⁴). Our findings suggest
231 that natural aerosol-climate feedbacks may play a role in moderating net
232 temperature response to CO₂-driven or other external forcings, and should be
233 included in fully-coupled simulations of past and future climate.

234

235

236

237

238

239

240

241

242

243

244

245

246

247 **References**

248

- 249 1 Arneeth, A. *et al.* Terrestrial biogeochemical feedbacks in the climate system.
250 *Nat. Geosci.* **3**, 525-532, doi:10.1038/ngeo905 (2010).
- 251 2 Carslaw, K. S. *et al.* A review of natural aerosol interactions and feedbacks
252 within the Earth system. *Atmos. Chem. Phys.* **10**, 1701-1737,
253 doi:10.5194/acp-10-1701-2010 (2010).
- 254 3 Hallquist, M. *et al.* The formation, properties and impact of secondary organic
255 aerosol: current and emerging issues. *Atmos. Chem. Phys.* **9**, 5155-5236
256 (2009).
- 257 4 Poschl, U. *et al.* Rainforest Aerosols as Biogenic Nuclei of Clouds and
258 Precipitation in the Amazon. *Science* **329**, 1513-1516,
259 doi:10.1126/science.1191056 (2010).
- 260 5 Martin, S. T. *et al.* SOURCES AND PROPERTIES OF AMAZONIAN
261 AEROSOL PARTICLES. *Reviews of Geophysics* **48**,
262 doi:10.1029/2008rg000280 (2010).
- 263 6 Martin, S. T. *et al.* Introduction: Observations and Modeling of the Green
264 Ocean Amazon (GoAmazon2014/5). *Atmos. Chem. Phys.* **16**, 4785-4797,
265 doi:10.5194/acp-16-4785-2016 (2016).
- 266 7 Andreae, M. O. *et al.* The Amazon Tall Tower Observatory (ATTO): overview
267 of pilot measurements on ecosystem ecology, meteorology, trace gases, and
268 aerosols. *Atmos. Chem. Phys.* **15**, 10723-10776, doi:10.5194/acp-15-10723-
269 2015 (2015).
- 270 8 Goldstein, A. H., Koven, C. D., Heald, C. L. & Fung, I. Y. Biogenic carbon and
271 anthropogenic pollutants combine to form a cooling haze over the
272 southeastern United States. *Proceedings of the National Academy of
273 Sciences of the United States of America* **106**, 8835-8840,
274 doi:10.1073/pnas.0904128106 (2009).
- 275 9 Spracklen, D. V. *et al.* Wildfires drive interannual variability of organic carbon
276 aerosol in the western US in summer. *Geophys. Res. Lett.* **34**,
277 doi:10.1029/2007gl030037 (2007).
- 278 10 Tunved, P. *et al.* High natural aerosol loading over boreal forests. *Science*
279 **312**, 261-263, doi:10.1126/science.1123052 (2006).
- 280 11 Twomey, S. Aerosols, clouds and radiation. *Atmospheric Environment* **25**,
281 2435-2442 (1991).
- 282 12 Rap, A. *et al.* Natural aerosol direct and indirect radiative effects. *Geophys.
283 Res. Lett.* **40**, 3297-3301, doi:10.1002/grl.50441 (2013).
- 284 13 Satheesh, S. K. & Moorthy, K. K. Radiative effects of natural aerosols: A
285 review. *Atmospheric Environment* **39**, 2089-2110,
286 doi:10.1016/j.atmosenv.2004.12.029 (2005).

- 287 14 Scott, C. E. *et al.* The direct and indirect radiative effects of biogenic
288 secondary organic aerosol. *Atmos. Chem. Phys.* **14**, 447-470,
289 doi:10.5194/acp-14-447-2014 (2014).
- 290 15 Unger, N. Human land-use-driven reduction of forest volatiles cools global
291 climate. *Nat. Clim. Chang.* **4**, 907-910, doi:10.1038/nclimate2347 (2014).
- 292 16 Spracklen, D. V. *et al.* Impacts of climate change from 2000 to 2050 on
293 wildfire activity and carbonaceous aerosol concentrations in the western
294 United States. *J. Geophys. Res.-Atmos.* **114**, doi:10.1029/2008jd010966
295 (2009).
- 296 17 Ward, D. S. *et al.* The changing radiative forcing of fires: global model
297 estimates for past, present and future. *Atmos. Chem. Phys.* **12**, 10857-10886,
298 doi:10.5194/acp-12-10857-2012 (2012).
- 299 18 Jolly, W. M. *et al.* Climate-induced variations in global wildfire danger from
300 1979 to 2013. *Nat. Commun.* **6**, 11, doi:10.1038/ncomms8537 (2015).
- 301 19 Heald, C. L. *et al.* Predicted change in global secondary organic aerosol
302 concentrations in response to future climate, emissions, and land use change.
303 *J. Geophys. Res.-Atmos.* **113**, 16, doi:10.1029/2007jd009092 (2008).
- 304 20 Mahowald, N. M. *et al.* Change in atmospheric mineral aerosols in response
305 to climate: Last glacial period, preindustrial, modern, and doubled carbon
306 dioxide climates. *J. Geophys. Res.-Atmos.* **111**, 22,
307 doi:10.1029/2005jd006653 (2006).
- 308 21 Charlson, R. J., Lovelock, J. E., Andreae, M. O. & Warren, S. G. OCEANIC
309 PHYTOPLANKTON, ATMOSPHERIC SULFUR, CLOUD ALBEDO AND
310 CLIMATE. *Nature* **326**, 655-661, doi:10.1038/326655a0 (1987).
- 311 22 Kulmala, M. *et al.* A new feedback mechanism linking forests, aerosols, and
312 climate. *Atmos. Chem. Phys.* **4**, 557-562 (2004).
- 313 23 Lihavainen, H., Asmi, E., Aaltonen, V., Makkonen, U. & Kerminen, V. M.
314 Direct radiative feedback due to biogenic secondary organic aerosol
315 estimated from boreal forest site observations. *Environ. Res. Lett.* **10**, 8,
316 doi:10.1088/1748-9326/10/10/104005 (2015).
- 317 24 Paasonen, P. *et al.* Warming-induced increase in aerosol number
318 concentration likely to moderate climate change. *Nat. Geosci.* **6**, 438-442,
319 doi:10.1038/ngeo1800 (2013).
- 320 25 Dusek, U. *et al.* Size Matters More Than Chemistry for Cloud-Nucleating
321 Ability of Aerosol Particles. *Science* **312**, 1375-1378,
322 doi:10.1126/science.1125261 (2006).
- 323 26 Mann, G. W. *et al.* Description and evaluation of GLOMAP-mode: a modal
324 global aerosol microphysics model for the UKCA composition-climate model.
325 *Geoscientific Model Development* **3**, 519-551, doi:10.5194/gmd-3-519-2010
326 (2010).
- 327 27 Lohmann, U. & Feichter, J. Global indirect aerosol effects: a review. *Atmos.*
328 *Chem. Phys.* **5**, 715-737 (2005).
- 329 28 van der Werf, G. R. *et al.* Global fire emissions and the contribution of
330 deforestation, savanna, forest, agricultural, and peat fires (1997-2009).

- 331 *Atmos. Chem. Phys.* **10**, 11707-11735, doi:10.5194/acp-10-11707-2010
332 (2010).
- 333 29 Guenther, A. B. *et al.* The Model of Emissions of Gases and Aerosols from
334 Nature version 2.1 (MEGAN2.1): an extended and updated framework for
335 modeling biogenic emissions. *Geoscientific Model Development* **5**, 1471-
336 1492, doi:10.5194/gmd-5-1471-2012 (2012).
- 337 30 Voulgarakis, A. *et al.* Interannual variability of tropospheric trace gases and
338 aerosols: The role of biomass burning emissions. *J. Geophys. Res.-Atmos.*
339 **120**, 7157-7173, doi:10.1002/2014jd022926 (2015).
- 340 31 Alves, E. G. *et al.* Seasonality of isoprenoid emissions from a primary
341 rainforest in central Amazonia. *Atmos. Chem. Phys.* **16**, 3903-3925 (2016).
- 342 32 Jardine, K. J. *et al.* Monoterpene 'thermometer' of tropical forest-atmosphere
343 response to climate warming. *Plant, Cell & Environment* **40**, 441-452,
344 doi:10.1111/pce.12879 (2017).
- 345 33 Jardine, A. B. *et al.* Highly reactive light-dependent monoterpenes in the
346 Amazon. *Geophys. Res. Lett.* **42**, 1576-1583, doi:10.1002/2014GL062573
347 (2015).
- 348 34 van der Werf, G. R., Randerson, J. T., Giglio, L., Gobron, N. & Dolman, A. J.
349 Climate controls on the variability of fires in the tropics and subtropics. *Glob.*
350 *Biogeochem. Cycle* **22**, 13, doi:10.1029/2007gb003122 (2008).
- 351 35 Tsigaridis, K., Lathiere, J., Kanakidou, M. & Hauglustaine, D. A. Naturally
352 driven variability in the global secondary organic aerosol over a decade.
353 *Atmos. Chem. Phys.* **5**, 1891-1904 (2005).
- 354 36 Myhre, G. *et al.* Radiative forcing of the direct aerosol effect from AeroCom
355 Phase II simulations. *Atmos. Chem. Phys.* **13**, 1853-1877, doi:10.5194/acp-
356 13-1853-2013 (2013).
- 357 37 Zhu, Z. C. *et al.* Greening of the Earth and its drivers. *Nat. Clim. Chang.* **6**,
358 791-795, doi:10.1038/nclimate3004 (2016).
- 359 38 Zaehle, S., Jones, C. D., Houlton, B., Lamarque, J. F. & Robertson, E.
360 Nitrogen Availability Reduces CMIP5 Projections of Twenty-First-Century
361 Land Carbon Uptake. *Journal of Climate* **28**, 2494-2511, doi:10.1175/jcli-d-13-
362 00776.1 (2015).
- 363 39 Kloster, S. & Lasslop, G. Historical and future fire occurrence (1850 to 2100)
364 simulated in CMIP5 Earth System Models. *Glob. Planet. Change* **150**, 58-69,
365 doi:10.1016/j.gloplacha.2016.12.017 (2017).
- 366 40 Hantson, S. *et al.* The status and challenge of global fire modelling.
367 *Biogeosciences* **13**, 3359-3375, doi:10.5194/bg-13-3359-2016 (2016).
- 368 41 Zhao, D. F. *et al.* Environmental conditions regulate the impact of plants on
369 cloud formation. *Nat. Commun.* **8**, 8, doi:10.1038/ncomms14067 (2017).
- 370 42 Heald, C. L. & Spracklen, D. V. Land Use Change Impacts on Air Quality and
371 Climate. *Chem. Rev.* **115**, 4476-4496, doi:10.1021/cr500446g (2015).
- 372 43 Spracklen, D. V. & Rap, A. Natural aerosol-climate feedbacks suppressed by
373 anthropogenic aerosol. *Geophys. Res. Lett.* **40**, 5316-5319,
374 doi:10.1002/2013gl057966 (2013).

375 44 Thackeray, C. W. & Fletcher, C. G. Snow albedo feedback: Current
376 knowledge, importance, outstanding issues and future directions. *Prog. Phys.*
377 *Geogr.* **40**, 392-408, doi:10.1177/0309133315620999 (2016).

378

379

380 **Acknowledgements**

381 We acknowledge support from the Natural Environment Research Council
382 (NE/K015966/1) and EU Horizon 2020 (SC5-01-2014; grant agreement no 641816).

383 This work used the ARCHER UK National Supercomputing Service

384 (<http://www.archer.ac.uk>).

385 **Author contributions**

386 All authors contributed to the research design. CS and SM performed model
387 simulations. AA and PP provided observational data. CS, DS and SA analysed the
388 data. All authors contributed to scientific discussions and helped to write the
389 manuscript.

390 **Additional information**

391 Supplementary information is available in the online version of the paper.

392 Correspondence and requests for materials should be sent to CS.

393 **Competing financial interests**

394 The authors declare no competing financial interests.

395 **Figure captions**

396 **Figure 1. Relationship between particle number anomaly and temperature**

397 **anomaly.** The particle number anomaly is for particles greater than 100 nm diameter
398 (N_{100}). Winter (top panels: a, b) and summer (bottom panels: c, d) are shown for
399 observations (left: a, c) and model (right: b, d). Each observation is represented by a

400 point (left), whilst the lines represent the median N_{100} anomaly per 2 K temperature
401 anomaly bin. Different locations are indicated by the different lines (see key). All
402 stations except one are in the Northern Hemisphere where winter is December to
403 February and summer is July to August. For the one station in the Southern
404 Hemisphere we show July to August as winter and December to February as
405 summer.

406 **Figure 2. Interannual variability in aerosol radiative effect (RE).** (a, b) Direct
407 radiative effect, (c, d) aerosol indirect effect shown for biogenic SOA (a, c) and fire
408 (b, d). Numbers on the panels show the standard deviation in global annual mean
409 RE over the period 1997 - 2007.

410 **Figure 3. Relationship between aerosol radiative effect (RE) and global**
411 **temperature anomaly.** (a) Direct radiative effect, (b) aerosol indirect effect shown
412 for biogenic SOA (blue) and fire (red). Symbols show results for the extra-tropics
413 ($>20^{\circ}\text{N}$ and $>20^{\circ}\text{S}$). Linear fits are shown for the extra-tropics (solid line) and at the
414 global scale (dashed line). Number on panel shows correlation (r) between RE and
415 temperature anomaly. Temperature anomalies are calculated relative to a 1971 to
416 2000 climatology.

417 **Figure 4. Simulated natural aerosol feedback.** Values are shown for biogenic
418 SOA (blue) and fire (red). Solid bars show the extra-tropical feedback ($>20^{\circ}\text{N}$ and
419 $>20^{\circ}\text{S}$), dashed bars show the global feedback. Error bar shows standard error in
420 the estimated feedback (based on 500 bootstrap samples).

421 **Methods**

422 **Observations:** We used long term observations of the number concentration of
423 particles larger than 100 nm in diameter (N_{100}) and surface temperature from 11

424 surface stations. The observations are as described in ref.²⁴. We de-seasonalised
425 both N_{100} and temperature through subtracting the long-term monthly mean from the
426 original data. We calculated the sensitivity of N_{100} to surface temperature between an
427 anomaly of -10 K and +10 K.

428 **Aerosol model:** We used the TOMCAT chemical transport model coupled to the
429 GLOMAP-mode aerosol microphysics model²⁶ to simulate the distribution of
430 atmospheric aerosol over the period 1997-2007. Fire emissions were from GFEDv3,
431 based on burned area, active fire detections and plant productivity from the
432 MODerate resolution Imaging Spectroradiometer (MODIS)²⁸. Emissions of isoprene
433 and monoterpenes were calculated using MEGANv2.1 (ref.²⁹) in the Community
434 Land Model (CLMv4.5). Emissions depend on the distribution of vegetation, CO_2
435 concentration, solar radiation, temperature and moisture. Anthropogenic aerosol
436 emissions and precursors were from the MACCity dataset⁴⁵. Other natural aerosol
437 and aerosol precursor emissions include oceanic DMS emissions calculated using a
438 sea-air transfer velocity⁴⁶ and a sea surface concentration database⁴⁷, sea-spray
439 emissions⁴⁸ and volcanic sulphur emissions⁴⁹. GLOMAP was forced with ERA-
440 Interim analyses from the European Centre for Medium Range Weather Forecasts
441 (ECMWF). We use offline oxidant concentrations from the TOMCAT chemical
442 transport model. Here GLOMAP has a horizontal resolution of $2.8^\circ \times 2.8^\circ$ and 31
443 vertical levels between the surface and 10 hPa. The model simulates aerosol
444 component mass and number concentration (two-moment modal) in seven
445 lognormal modes: hygroscopic nucleation, Aitken, accumulation, coarse, and non-
446 hygroscopic Aitken, accumulation and coarse modes. The modal version of the
447 model matches a more computationally expensive sectional scheme⁵⁰. Secondary
448 organic aerosol (SOA) is formed from the oxidation of monoterpenes and isoprene

449 and is treated as described in ref.¹⁴. The oxidation products of monoterpenes are
450 able to participate in new particle formation⁵¹ and growth whereas the oxidation
451 products of isoprene contribute only to condensational growth. A control simulation
452 where emissions and meteorology varied according to simulation year was
453 compared against simulations where one specific emission or process was fixed to
454 1997 values. These were a) anthropogenic emissions, b) biogenic VOC emissions,
455 c) landscape fire emissions, d) ERA-Interim fields. All simulations were run for the
456 period 1997 to 2007.

457 **Radiation model:** Top-of-atmosphere, all-sky aerosol radiative effects (RE) were
458 calculated using the Suite of Community Radiative Transfer codes (SOCRATES)⁵².
459 We calculated the direct radiative effect (DRE) and the aerosol indirect effect (AIE)
460 resulting from changes to cloud droplet number concentration. Full details are
461 provided in ref.¹⁴.

462 Aerosol RE were calculated for all five aerosol model simulations that are described
463 above. The global annual mean RE was calculated for each simulation. The anomaly
464 in global annual mean radiative effect was calculated with respect to the start year of
465 the simulation (1997). We then calculated global annual mean RE anomaly for each
466 emission or process as the difference in global mean RE anomaly between the
467 control simulation and the simulation where that process had been fixed to 1997
468 values. The sum of RE anomaly from the four simulations agreed with the RE
469 anomaly from the control simulation to within 2%.

470 **Climate feedback:** Global annual temperature anomalies (ΔT) are from the National
471 Oceanic and Atmospheric Administration (NOAA). We used the NOAA Merged Land
472 Ocean Global Surface Temperature Analysis Dataset (NOAAGlobalTemp v4.0.1)⁵³,
473 a spatially gridded ($5^\circ \times 5^\circ$) global surface temperature dataset. Temperature

474 anomalies were calculated over land and ocean with respect to the 1971 to 2000
475 climatology. The Pearson's correlation (r) between ΔRE and ΔT was calculated for
476 each simulation.

477 We calculate the climate feedback (λ) following previous work¹. Climate feedbacks,
478 expressed in units of $W m^{-2} K^{-1}$, are calculated for each natural aerosol as the
479 change in top-of-atmosphere radiative effect (ΔRE) divided by the change in global
480 mean surface temperature (ΔT) (i.e., $\lambda = \Delta RE / \Delta T$), determined from the gradient of
481 the best fit line between the ΔRE and ΔT . Uncertainty in the calculated feedback is
482 estimated using a bootstrapping approach, based on 500 bootstrap samples.

483 **Data availability:** The NOAA Merged Land Ocean Global Surface Temperature
484 Analysis Dataset (NOAAGlobalTemp v4.0.1) is available online
485 ([https://www.ncdc.noaa.gov/data-access/marineocean-data/noaa-global-surface-
486 temperature-noaaglobaltemp](https://www.ncdc.noaa.gov/data-access/marineocean-data/noaa-global-surface-temperature-noaaglobaltemp)). Data from our model simulations are available upon
487 request.

488 **Code availability:** A request for the code used to generate these results can be
489 made via http://www.ukca.ac.uk/wiki/index.php/Main_Page

490

491

492 45 Granier, C. *et al.* Evolution of anthropogenic and biomass burning emissions
493 of air pollutants at global and regional scales during the 1980-2010 period.
494 *Clim. Change* **109**, 163-190, doi:10.1007/s10584-011-0154-1 (2011).

495 46 Nightingale, P. D. *et al.* In situ evaluation of air-sea gas exchange
496 parameterizations using novel conservative and volatile tracers. *Glob.*
497 *Biogeochem. Cycle* **14**, 373-387, doi:10.1029/1999GB900091 (2000).

498 47 Kettle, A. J. & Andreae, M. O. Flux of dimethylsulfide from the oceans: A
499 comparison of updated data sets and flux models. *Journal of Geophysical*
500 *Research: Atmospheres* **105**, 26793-26808, doi:10.1029/2000JD900252
501 (2000).

- 502 48 Gong, S. L. A parameterization of sea-salt aerosol source function for sub-
503 and super-micron particles. *Glob. Biogeochem. Cycle* **17**, 1097,
504 doi:10.1029/2003GB002079 (2003).
- 505 49 Dentener, F. *et al.* Emissions of primary aerosol and precursor gases in the
506 years 2000 and 1750 prescribed data-sets for AeroCom. *Atmos. Chem. Phys.*
507 **6**, 4321-4344, doi:10.5194/acp-6-4321-2006 (2006).
- 508 50 Mann, G. W. *et al.* Intercomparison of modal and sectional aerosol
509 microphysics representations within the same 3-D global chemical transport
510 model. *Atmos. Chem. Phys.* **12**, 4449-4476, doi:10.5194/acp-12-4449-2012
511 (2012).
- 512 51 Metzger, A. *et al.* Evidence for the role of organics in aerosol particle
513 formation under atmospheric conditions. *Proceedings of the National*
514 *Academy of Sciences of the United States of America* **107**, 6646-6651,
515 doi:10.1073/pnas.0911330107 (2010).
- 516 52 Edwards, J. M. & Slingo, A. Studies with a flexible new radiation code .1.
517 Choosing a configuration for a large-scale model. *Q. J. R. Meteorol. Soc.* **122**,
518 689-719, doi:10.1002/qj.49712253107 (1996).
- 519 53 Smith, T. M., Reynolds, R. W., Peterson, T. C. & Lawrimore, J. Improvements
520 to NOAA's Historical Merged Land–Ocean Surface Temperature Analysis
521 (1880–2006). *Journal of Climate* **21**, 2283-2296, doi:10.1175/2007jcli2100.1
522 (2008).

523

524

525

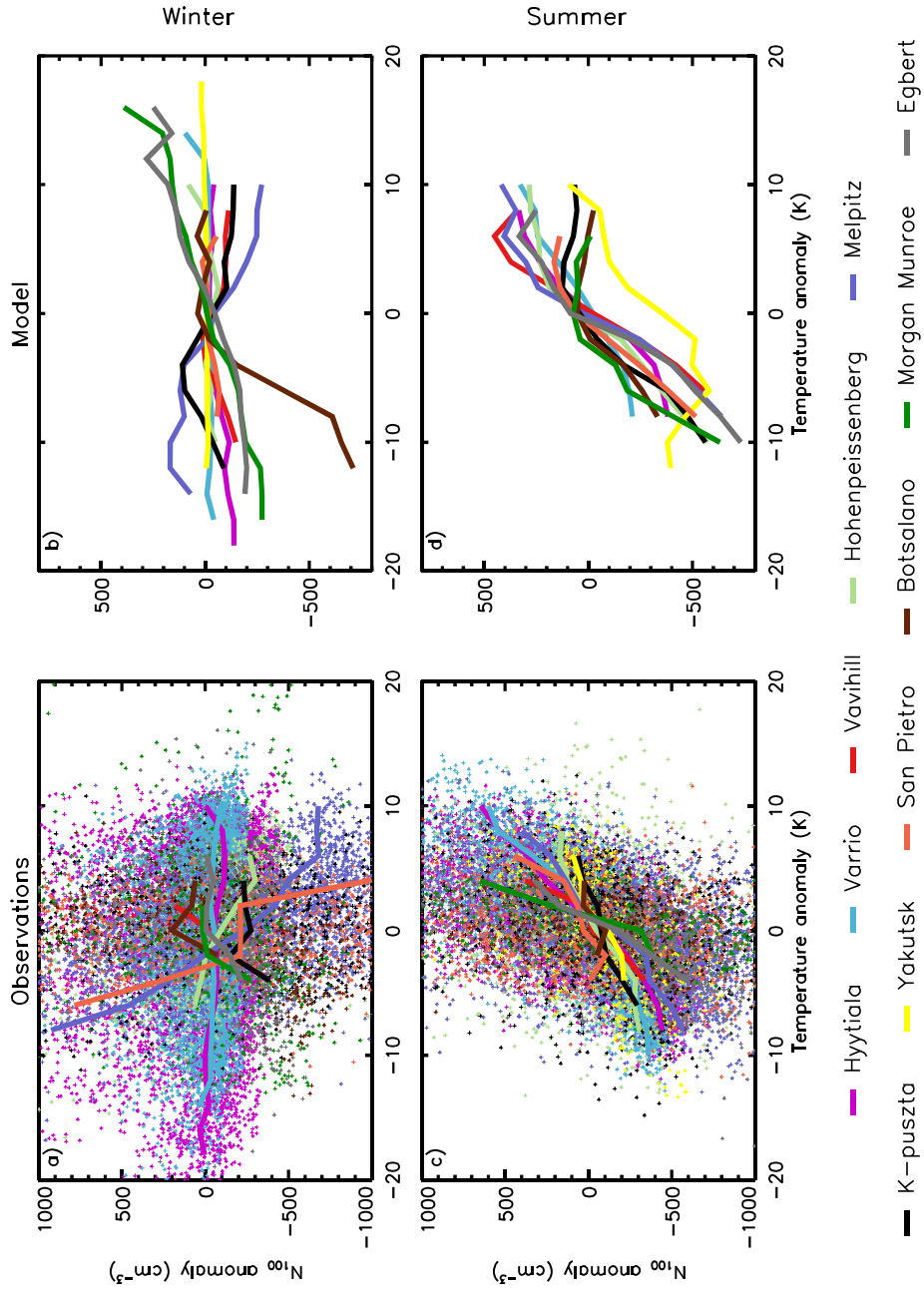
526

527

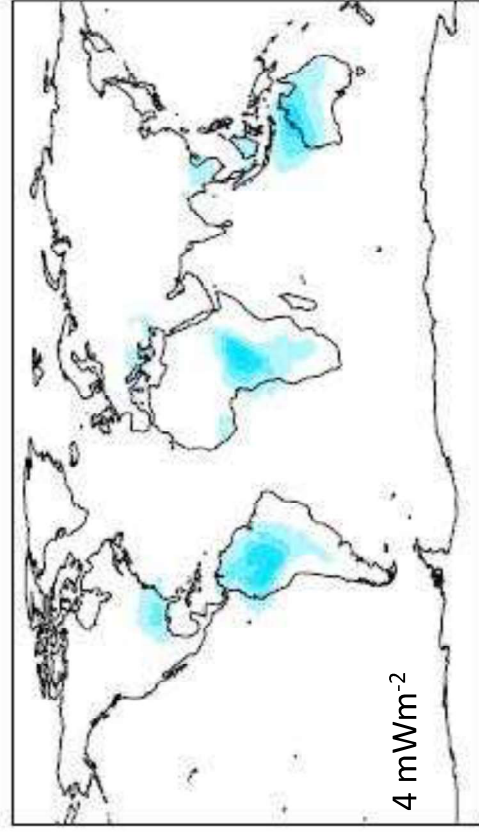
528

529

530

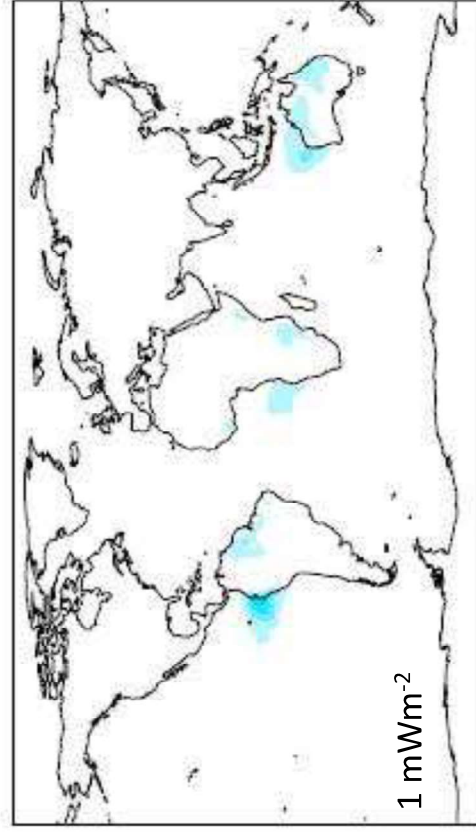


(a)



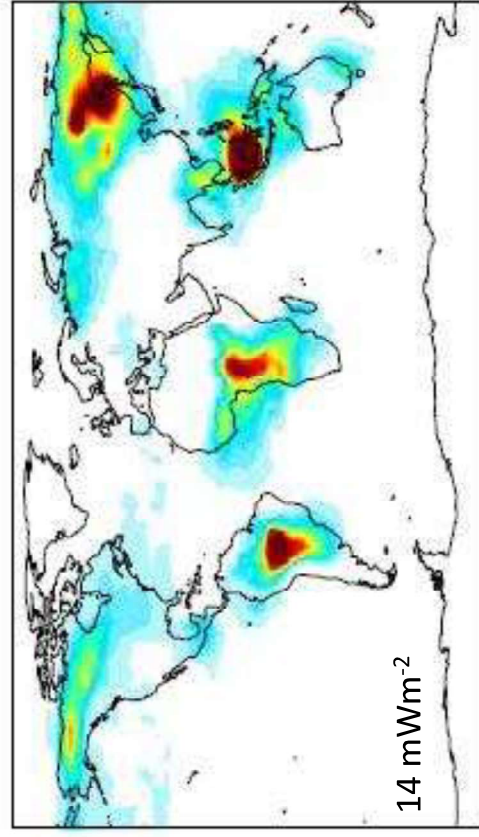
0.00 0.10 0.20 0.30 0.40 0.50 Wm⁻²

(c)



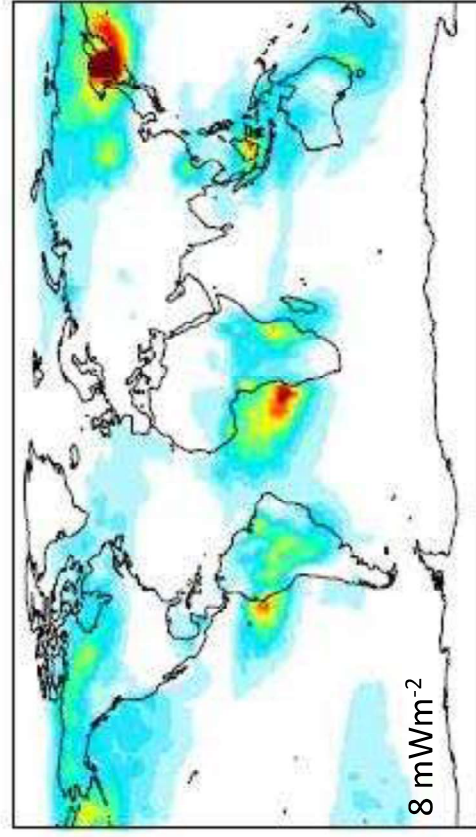
0.00 0.05 0.10 0.15 0.20 0.25 Wm⁻²

(b)



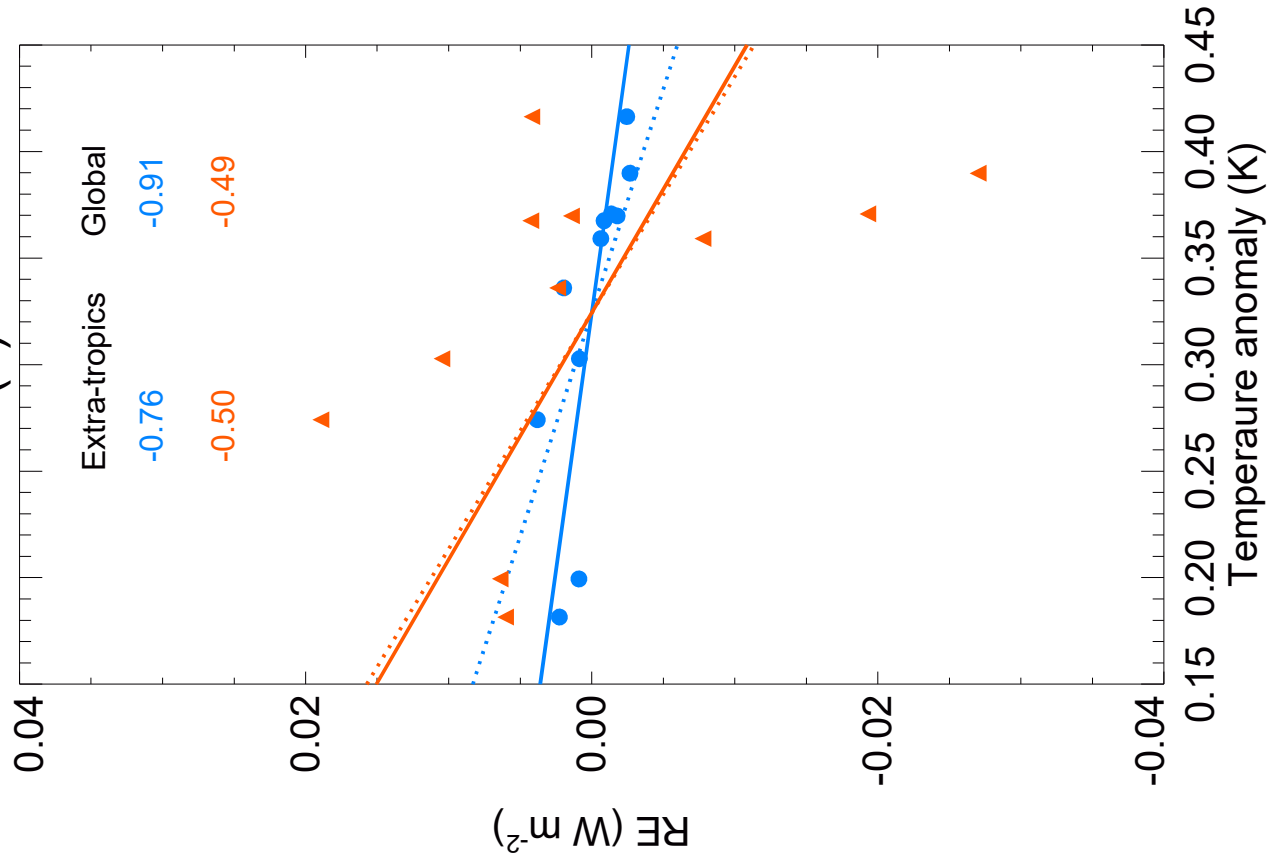
0.00 0.10 0.20 0.30 0.40 0.50 Wm⁻²

(d)



0.00 0.05 0.10 0.15 0.20 0.25 Wm⁻²

(a)



(b)

